European Commission

JRC TECHNICAL REPORTS

In vitro methods for Nrf2 pathway induction

Evaluation of the rotenone-induced activation of the Nrf2 pathway in a stem cell-derived neuronal model

Pistollato Francesca, Juan Casado-Poblador, Anna Bal-Price

2016

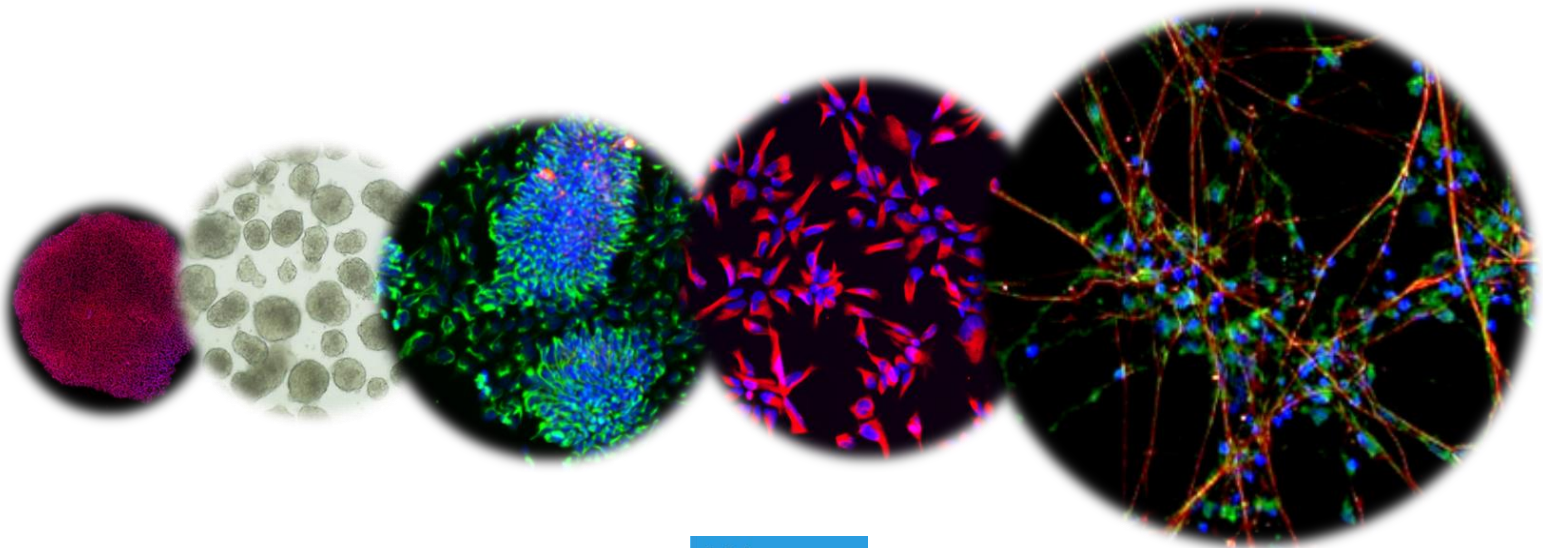

Joint Research Centre

EUR 28172 EN

Contact information
Name: Anna Bal-Price
Address: Directorate General Joint Research Centre, Directorate F – Health, Consumers and Reference Materials, Via E. Fermi, 2749, I-21027 Ispra (VA)
E-mail: anna.price@ec.europa.eu
Tel.: +39 0332 786018

JRC Science Hub
https://ec.europa.eu/jrc

JRC103676

EUR 28172 EN

PDF ISBN 978-92-79-63194-8 ISSN 1831-9424 doi:10.2787/36841

Luxembourg: Publications Office of the European Union, 2016

How to cite: Pistollato Francesca, Juan Casado-Poblador, Anna Bal-Price. In vitro methods for Nrf2 pathway induction: Evaluation of the rotenone-induced activation of the Nrf2 pathway in a stem cell-derived neuronal model. EUR 28172 EN; doi: 10.2787/36841

Table of contents

Abstract

Oxidative stress is one of the cellular responses determined at early stages of toxicity and can be induced by many different classes of chemicals. The nuclear factor (erythroid-derived 2)-like 2 (Nrf2) represents one of the key regulators of the Antioxidant-Response-Element-(ARE)-driven cellular defence mechanisms against oxidative stress. Nrf2 has been shown to have a cytoprotective, antioxidant and anti-inflammatory role in virtually all cell types in the body, both under physiological and disease conditions, as it regulates the expression of enzymes involved in detoxification processes. The SCR&Tox consortium, part of the SEURAT-1 research initiative, established to investigate Nrf2 signaling activation in neuronal models derived from hiPSCs. Analysis of Nrf2 signaling activation could serve as a base for the establishment of a horizontal assay to assess oxidative stress induction. Neuronal and glial cells undergo oxidative stress as an early response to different classes of chemicals, including inhibitors of mitochondrial respiration, such as rotenone, which is known to inhibit complex I of the mitochondrial respiratory chain. Moreover, human induced pluripotent stem cells (hiPSCs) are currently regarded as a powerful tool for drug and chemical screening and development of new in vitro testing strategies in the field of toxicology, including neurotoxicity and developmental neurotoxicity evaluation.

This technical report summarizes the strategy adopted by EURL-ECVAM to assess Nrf2 signalling activation in neuronal models derived from hiPSCs. In particular, as agreed within the SCR&Tox consortium, two hiPSC-neuronal models were used: (i) an Nrf2-Luciferase reporter neural stem cell model (called Clone 27 (Cl27), obtained from Phenocell, France), and (ii) a wild type IMR90-hiPSC-derived neuronal/glial model (obtained from I-Stem, France). The results obtained with the wild type (IMR90-hiPSC) neuronal model indicate that rotenone induces the activation of Nrf2 signaling, increases the number of astroglial cells and decreases the number of dopaminergic neurons. The obtained results suggest that hiPSC-derived mixed neuronal/glial culture could be a valuable in vitro model for the establishment of neuronal specific assays to evaluate Nrf2 pathway activation (biomarker of oxidative stress) using neuronal specific readouts that could be applied to in vitro neurotoxicity evaluation.

1 Introduction

In recent years (2011-2015), the European Union Reference Laboratory for Alternative to Animal Testing (EURL ECVAM) and the "Health, Chemicals Safety and Alternative Methods" Unit (former Systems Toxicology Unit) of the Joint Research Centre's Directorate F "Consumers and Reference Materials" (former Institute for Health and Consumer Protection) have been involved in the SEURAT-1 initiative (http://www.seurat-1.eu/), aimed at developing knowledge and technology building blocks required for the development of solutions for the replacement, reduction or refinement (3Rs) of current repeated dose systemic toxicity testing in vivo used for the assessment of human safety. The SEURAT-1 research initiative was composed of six research projects (SCR&Tox, HeMiBio, DETECTIVE, COSMOS, NOTOX and ToxBank), coordinated and supported by a 7th project (COACH). Among these projects, SCR&Tox (http://www.scrtox.eu/) aimed at making use of human pluripotent stem cell lines, in particular human induced pluripotent stem cells (hiPSCs) and their derivatives, to provide in vitro assays for predicting toxicity of pharmaceutical compounds and cosmetic ingredients.

HiPSCs represent unique tools for toxicity screening and improving mechanistic understanding of chemically-induced adverse effects (Hou et al., 2013; Kumar et al., 2012; Yap et al., 2015). HiPSCs have been identified as a potential source of various cell types for toxicity testing (Hou et al., 2013). HiPSCs share similar characteristics with human embryonic stem cells (hESCs) (Krueger et al., 2010; Pistollato et al., 2012), i.e. are characterized by unlimited self-renewal and capacity to generate different human tissue-specific somatic cells (Avior et al., 2016; Robinton and Daley, 2012), including neurons and glia. Moreover, these stem cell-based systems offer an innovative alternative for obtaining a large number of human cells, serving as a valuable tool for the development of in vitro models for toxicity testing (Avior et al., 2016), often applicable for high throughput screening (HTS) approaches (Desbordes and Studer, 2013).

Oxidative stress is one of the non-cell specific cellular responses determined at early stages of toxicity and induced by different classes of chemicals. Among the key regulators of the Antioxidant-Response-Element-(ARE)-driven cellular defence mechanisms against oxidative stress is the Nuclear factor (erythroid-derived 2)-like 2 (Nrf2), which has a cytoprotective role in several diseases (Ramsey et al., 2007). Under normal (unstressed) conditions, Nrf2 is kept in the cytoplasm by Kelch like-ECH-associated protein 1 (Keap1) and Cullin 3, which degrade Nrf2 by ubiquitination (Sun et al., 2007). Under oxidative/electrophilic stress, cysteine residues in Keap1 get disrupted, Nrf2 travels to the nucleus, binds to the antioxidant response element (ARE) in the upstream promoter region of many antioxidative genes (e.g., NQO1, SRXN1, GSR, HMOX1) that support detoxification processes that take place in many neurodegenerative diseases (Ramsey et al., 2007). Within the SCR&Tox consortium, it was decided to assess Nrf2 signaling activation in neuronal models derived from hiPSCs. Analysis of Nrf2 signaling activation could serve as a base for the establishment of a horizontal assay, relevant to different organ toxicity, permitting assessment of oxidative stress induction.

In our studies we exposed cells to rotenone that is a specific inhibitor of mitochondrial complex I, triggering oxidative stress (positive control). Rotenone is a crystalline isoflavone (Figure 1) used as a broad-spectrum insecticide, piscicide, and pesticide, occurring naturally in the seeds and stems of several plants, such as the jicama vine plant and the roots of several members of Fabaceae.

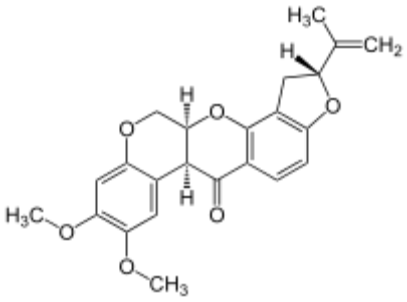

Figure 1. Skeletal formula of rotenone

It is classified as moderately hazardous by the World Health Organization[1]. Rotenone works by inhibiting the transfer of electrons from iron-sulfur centres in complex I to ubiquinone in the mitochondrial respiratory chain. This creates a back-up of electrons within the mitochondrial matrix, causing reduction of cellular oxygen and the generation of reactive oxygen species (ROS). Rotenone has been shown to cause oxidative stress triggering the translocation of Nrf2 from the cytoplasm into the nucleus, followed by induction of the Nrf2-ARE target gene transcription (Tufekci et al., 2011).

Importantly, environmental exposure to rotenone has been shown to be linked to an increase risk of Parkinson's disease (PD) and PD-like neuropathology, as shown by several human epidemiological studies (Nandipati and Litvan, 2016).

This technical report summarizes the strategy adopted by EURL-ECVAM to assess Nrf2 signalling activation in neuronal models derived from hiPSCs and the main results. To assess the effects of rotenone on Nrf2 pathway activation, two hiPSC-neuronal models were adopted: a Nrf2-Luciferase reporter neural stem cell model (Cl27, obtained from Phenocell, France, one of the partners contributing to the SCR&Tox project), and a wild type IMR90-hiPSC-derived neuronal/glial model (kindly provided by Dr. Marc Peschanski (Coordinator of SCR&Tox), I-Stem, France).

Overall our results suggest that hiPSC-derived mixed neuronal/glial culture could be a valuable in vitro model for the establishment of an assay for evaluation of Nrf2 pathway activation (a biomarker of oxidative stress) combined with other test methods for perturbation of neuronal-specific pathways, which could be applied to assess neurotoxicity in vitro.

2 Methodological approach

Rotenone was used to assess the activation of the Nrf2 pathway in mixed cultures of neuronal and glial cells differentiated from hiPSC-derived neural stem cells (NSCs). In particular two different cellular models have been used: an Nrf2-Luciferase reporter NSC model (called Cl27, obtained from Phenocell, France), and a wild type IMR90-hiPSC-derived neuronal/glial model (obtained from I-Stem, France). The maintenance and differentiation protocols applied for Cl27 were the ones specified by the supplier (PhenoCell), while maintenance, expansion and differentiation protocols for IMR90-hiPSCs were developed and optimized in house and are available at https://ecvam-dbalm.jrc.ec.europa.eu/beta/index.cfm/methodsAndProtocols/index.

[1] IPCS, International Programme on Chemical Safety; United Nations Environment Programme; International Labour Organization; World Health Organization. (2007). The WHO Recommended Classification of Pesticides by Hazard. World Health Organization. ISBN 92-4-154663-8. Retrieved 2007-12-02.

A more detailed description of the cellular models and the readouts used to assess the effects of rotenone on Nrf2 pathway activation and on neuronal and glia-related endpoints are described in the next sections.

2.1 The cellular models: human induced pluripotent stem cell (hiPSC)-derived neuronal and glial cultures

2.1.1 Nrf2-Luciferase reporter (NSC) model (Clone 27)

An Nrf2-Luciferase reporter NSC model (named clone 27 (Cl27)) was created by Phenocell (http://phenocell.fr/), as part of the activities related to the SCR&Tox consortium, by transducing an Nrf2-Luciferase construct in NSCs derived from PC1429-hiPSCs (details about the transduction method can be obtained from PhenoCell). Cells were expanded and subcultured as indicated by manufacturer. The medium used for NSC expansion was composed of: 50% Neurobasal medium, 50% DMEM-F12 medium (with GlutaMax), B27 supplements (without retinol), N2 supplements, Beta-mercaptoethanol (50 µM), and adding basic fibroblast growth factor (bFGF) (10 ng/ml), epidermal growth factor (EGF) (10 ng/ml) and brain derived neurotrophic factor (BDNF) (20 ng/ml) (all from ThermoFisher). Cl27 cells were differentiated for 21 days as recommended by Phenocell using the same medium formulation, plus BDNF (20 ng/ml), but withdrawing bFGF and EGF.

Cells were treated for either 24 or 72 hr with 1, 10, 100, 500 and 2500 nM rotenone (Sigma-Aldrich, dissolved in DMSO) at various differentiation stages (i.e., differentiation days 5, 12 and 19), accounting for solvent control analysis. Analysis of cytotoxicity (by Alamar blue test) and Nrf2/luciferase activity were assessed by means of a plate reader (Tecan) after 24 and 72 hr treatment. Further immunostaining and qPCR analyses were conducted to assess the phenotypic identity of the differentiated cells.

2.1.2 Wild type hiPSC-IMR90-derived neuronal/glial cells

IMR90-hiPSCs were kindly provided by Dr. Marc Peschanski (I-Stem, France). IMR90 fibroblast cell line was established on 07/07/1975 using explants of minced lung tissue obtained from a clinically normal 16 week old fetus and they exhibit a normal female karyotype (46, XX)[2]. IMR90 fibroblasts were reprogrammed into hiPSCs at I-Stem by viral transduction of Oct4 and Sox2 by using the pMIG vectors (Addgene).

hiPSCs were cultured, under feeder-free conditions, on matrigel™ hESC-qualified matrix (Corning) pre-coated Petri-dishes in the presence of mTeSR™1 medium containing mTeSR™1 5X supplements (Stem Cell Technologies) prepared following manufacturer's instructions. HiPSC colonies were passaged by micro-dissection using a 30G needle.

IMR90-hiPSCs were differentiated toward neurons and glia following a protocol described in https://ecvam-dbalm.jrc.ec.europa.eu/beta/index.cfm/methodsAndProtocols/index, which is a modified version of the method described by Pistollato et al. (Pistollato et al., 2014). Briefly, IMR90-derived colonies cultured on matrigel™ hESC-qualified matrix (Corning) coated dishes were manually microdissected into 200 µm x 200 µm fragments using a 30G needle. For the generation of embryoid bodies (EBs), fragments were transferred into a low attachment Petri-dish (Greiner) and cultures in EB medium. After 48 hours, generated EBs were plated on laminin (Sigma-Aldrich)-coated dishes and cultured in neuroepithelial induction (NRI) medium for further 7 days. On day 8, neuroepithelial aggregates (rosettes) were visible and were cut in fragments using a 30G needle under a phase contrast microscope. Then, rosettes were spun down, resuspended

[2] https://catalog.coriell.org/

in 1 ml of phosphate-buffered saline (PBS, 1X) and partially dissociated using a p1000 tip. Finally, dissociated rosettes were plated on laminin-coated dishes and cultured in the presence of neural differentiation (ND) medium for 3 weeks.

A protocol for the expansion of rosette-derived neural stem cells (NSCs) was developed (https://ecvam-dbalm.jrc.ec.europa.eu/beta/index.cfm/methodsAndProtocols/index). Briefly, rosette-derived NSCs were passaged by enzymatic dissociation using 0.05% Trypsin-EDTA (ThermoFisher), and replated on matrigel® basement membrane matrix (Corning) coated dishes in the presence of neural induction (NI) medium (50,000 cells/cm^2). NI medium was refreshed every other day. At early passages (1-4), a cell plating density of ~ $75x10^4$ cells/cm^2 was applied to improve cell viability after passaging. NSCs were differentiated into neuronal mixed cultures using ND medium as described above. On differentiation day 21, cells were treated for 24 hr with 1, 10, 100 nM rotenone (Sigma-Aldrich, dissolved in DMSO), accounting for solvent control analysis. For detailed information about the different media used for expansion and differentiation of NSCs, refer to recently published manuscript from Zagoura D. et al. (Zagoura D et al. 2016) and the EURL ECVAM DBALM website https://ecvam-dbalm.jrc.ec.europa.eu/methods-and-protocols/protocol/standard-operating-procedure-for-differentiation-of-human-induced-pluripotent-stem-cells-into-post-mitotic-neurons-and-glial-cells-%28mixed-culture%29-protocol-no.-165/key/p_1570 and https://ecvam-dbalm.jrc.ec.europa.eu/methods-and-protocols/protocol/standard-operating-procedure-for-expansion-of-rosette-derived-neural-stem-cells-protocol-no.-166/key/p_1571. A 24 hr treatment with 10 μM and 100 μM hydrogen peroxide (H2O2, Sigma-Aldrich) was used as a positive control for induction of oxidative stress and activation of the Nrf2 pathway.

2.2 Readouts applied to assess rotenone effects

Assessment of rotenone effects was assessed by performing the analyses described in the following sections.

2.2.1 Alamar blue (resazurin) for analysis of cell viability

Cl27 cells were exposed to different concentrations of rotenone (ranging from 1 nM to 2500 nM) for 72 hr to determine possible cytotoxic effects. To this end, the medium containing rotenone was removed and the cells were incubated with 10 μM resazurin (ThermoFisher), diluted in ND medium in the incubator (37°C, 5% CO_2) for 2 hr. Resazurin is the active ingredient of alamar blue reagent which upon entering live cells gets converted to resorufin that is red and highly fluorescent, and its absorbance can be read on a spectrophotometer. The fluorescence of the reagent was measured at 530-560 nm-/590 nm (excitation/emission) in a multiwell fluorimetric reader (Tecan). The results were normalized to the mean of solvent treated cells (0.1% DMSO).

2.2.2 Immunocytochemistry and high content imaging (HCI)

About 6000-7000 cells/well in 96 well plates were plated and differentiated for 21 days. On day 21 cells were treated with either rotenone or H2O2 as described above, and after 24 hr cells were fixed with cold 4% paraformaldehyde, washed in PBS 1X, permeabilized in PBS 1X containing 0.1% Triton-X-100 and 3% bovine serum albumin (BSA) for 15 minutes at room temperature, and further incubated with 3% BSA/1X PBS (blocking solution) to prevent nonspecific binding of the antibodies. The cells were then incubated with primary antibodies as follows: neurofilament 200 (NF200, rabbit, 1:1000, Sigma-Aldrich), glial fibrillary acidic protein (GFAP, mouse, 1:500, Merck-Millipore), microtubule-associated protein-2 (MAP2, mouse, 1:500, Sigma-Aldrich), synaptophysin (SYN, rabbit, 1:200, Abcam), Nrf2 (rabbit), Keap1 (rabbit), sulfiredoxin1 (SRXN1,

goat),NAD(P)H quinone oxidoreductase 1 (NQO1, goat) (all 1:200, Abcam), nestin (rabbit, 1:200, Sigma-Aldrich), Oct4 (mouse, 1:100, Millipore), Sox2 (rabbit, 1:200, Millipore), tyrosine hydroxylase (TH, rabbit, 1:200, Millipore), gamma-aminobutyric acid (GABA, mouse, 1:100, Sigma-Aldrich), vesicular glutamate transporter 1 (VGlut1, rabbit, 1:500, Abcam) in blocking solution overnight at 4°C. The cells were washed with PBS and further incubated with fluorochrome-conjugated secondary antibodies (1:1000, Invitrogen). Nuclei were counterstained with DAPI dye (0.3µM, Sigma-Aldrich). Quantification of mean fluorescence intensity and of the relative percentages of cell types was performed using two specific ArrayScan algorithms: Cytotoxicity V.4 and NucTrans V.4 bioapplications. Both the applications apply a specific nuclear mask around the DAPI staining defined according to nuclear morphology, discarding invalid nuclei (i.e., nuclei that were pyknotic, bright and/or dense clumps of cells) and, on the valid nuclei (i.e., homogenous round-shaped nuclei, indicative of live cells) an additional cell body shape mask was applied according to the type of antibody/antigen staining, as already described (O'Brien et al., 2006). The NucTrans V.4 algorithm calculates the level of fluorescence intensity both in the nucleus and the cytoplasm, applying respectively a circular mask (for nuclear signal) and a ring shape mask (for cytoplasmic signal). Secondary antibody incubation alone was used to determine the intensity level of fluorescent background that was subtracted. The ArrayScan™ XTI High Content Platform was set up to take a minimum of 20 pictures/well. Each staining was done on 7-8 internal replicates for each condition.

2.2.3 Quantitative real-time PCR (qPCR)

Analysis of gene expression by qPCR was performed on differentiated and rotenone-treated (i.e., 1-10-100 nM) and untreated (control) cells. RNA was isolated using the RNAqueous®-Micro Kit (ThermoFisher) according to manufacturer's instructions, and 500 ng of total RNA was reverse transcribed using the High Capacity cDNA Reverse Transcription Kit (as directed, ThermoFisher). qPCR reactions were run in duplicate using TaqMan® Gene Expression Master Mix (ThermoFisher) and the following TaqMan gene expression assays (all from ThermoFisher): NCAM1 (Hs00941830_m1), GFAP (Hs00909233_m1), MAP2 (Hs00258900_m1), NQO1 (Hs02512143_s1), SRXN1 (Hs00607800_m1), HMOX1 (Hs01110250_m1), GSR (Hs00167317_m1), PAX6 (Hs01088112_m1), NES (Hs00707120_s1), SOX1 (Hs01057642_s1), GRIA1 (Hs00181348_m1), GAP43 (Hs00967138_m1), GABRA3 (Hs00968132_m1), GABRA1 (Hs00168058_m1), NR4A2 (Hs00428691_m1), TH (Hs00165941_m1), GAPDH (Hs02758991_g1), ACTB (Hs99999903_m1). Fluorescent emission was recorded in real-time using the ABI PRISM Sequence Detection System 7900HT (Applied Biosystems). PCR amplification conditions consisted of 45 cycles with primers annealing at 60°C. Relative RNA quantities were normalized to the reference genes GAPDH and ACTB and untreated cells were used as a calibrating condition (ΔΔCt Method).

2.2.4 Electrophysiological measurements

Dissociated rosette-like structures (differentiation day 7) or NSCs derived from rosettes were plated on Multielectrode arrays (MEAs) ($1x10^5$ cells/MEA chip) containing complete ND medium and differentiated for 3 weeks as described above. At the end of differentiation, MEA plates were sealed with a semi-permeable membrane (standard MEAs) in a laminar flow hood to keep the cultures sterile for recording of the mean firing rate (MFR, number of spikes/min) . Each chip (single well) contains 60 microelectrodes, aligned in an 8 x 8 square grid, with the four corners missing. One of the electrodes can be replaced by one ground reference, allowing recording from the remaining 59 electrodes. All data represent the average of at least n=3 biological replicates. The measurements were performed with a MEA1060-Inv-BC-amplifier with integrated temperature process control adjusted to 37°C and 5% CO_2 and data were recorded with MC Rack software (Multichannel systems). Peaks from MEA raw data were detected

using threshold limit of −4.7 σ, where σ represents the standard deviation of the basal noise. From each MEA, the number of spikes/min and bursts/30 min were calculated (a burst was considered as a train of at least 2-5 action potentials occurring max every 100 millisec). Spike number data were normalized with respect to baseline activity for each MEA separately. Post-recording data were processed with NeuroExplorer (NexTechnologies) and Excel (Microsoft).

2.2.5 Measurements of Nrf2/Luciferase

Cl27 cells were seeded onto 96-well plates at a density of 50.000 cells/cm2 and treated with different concentrations of rotenone (from 1 to 2500 nM), with 100 μM H_2O_2 (both products from Sigma-Aldrich) serving as a positive control, and with DMSO as a negative control. The luciferase cell culture lysis reagent was used as a blank. After 24 or 72 hr of treatment, the medium was removed and 100 μL of cold PBS was added into each well. PBS was removed and cells were lysed in 20 μL of luciferase cell culture lysis reagent at room temperature and on a plate shaker for 10 min. 100 μL of Luciferase assay reagent was added into each well and determination of the luciferase activity was done following manufacturer's protocol (Promega, Madison, WI). The luciferase activity was measured by a Tecan plate reader. The data (considering 6 internal replicates per plate, and a total of 3 biological replicates) were expressed as fold induction over controls (i.e., either untreated cells or undifferentiated NSCs).

2.2.6 Statistical analysis

Statistical significance was assessed by one-way ANOVA with Dunnett's Multiple Comparison Test as Post Test, comparing all columns vs control (Ctr) column using the GraphPad Prism 5 software (http://www.graphpad.com/). All data represent the average of at least n=3 biological replicates ± standard error mean (S.E.M.). For all graphs, an asterisk over a bar indicates a significant difference with the control group, an asterisk over a bracket shows a significant difference as indicated. For all graphs, * $p < 0.05$, ** $p < 0.01$, *** $p < 0.001$.

3 Results

3.1 Effects of rotenone on Cl27 cells (Nrf2/Luciferase reporter model)

3.1.1 Neuronal and glial differentiation of Cl27 cells

First the effects of rotenone on Cl27-Nrf2/luciferase cells (generated by PhenoCell) at different stages of differentiation were assessed, to evaluate the activation of the Nrf2 pathway. As a preliminary step, the neuronal and glial differentiation potential of Cl27 cells was characterized by analysis of immunocytochemistry and qPCR.

Cl27 cells expanded efficiently, with a doubling time of ~ 2.5 days. However, some pluripotent stem-like cells appeared to be present and grow as tiny colonies that tended to expand over time (Figure 2A, B). Upon differentiation, Cl27 cells did not reach an advanced stage of differentiation, even when prolonging the differentiation time to 28 days, as shown by analysis of the NSC marker nestin (Figure 2C), which was expressed in nearly all cells after 21 days of differentiation, and analysis of Sox2 (Figure 2H), still visible in differentiated cell cultures. Additionally some cells resulted positive for the PSC

marker Oct4 (Figure 2H), even after 28 days of differentiation (Figure 2I). Nevertheless, despite their poorly differentiated appearance, Cl27 cells expressed classic neuronal markers (B-III-tubulin, MAP2, NF200) (Figure 2D-F), and some cells resulted positive for GFAP (indicative of astroglia) (Figure 2G).

qPCR analysis of the NSC-related genes Pax6, Sox1 and Nestin (Figure 2J) and of the neuronal gene NCAM1 (Figure 2K) showed no significant variations over time, while the neuronal related gene MAP2 (Figure 2K) resulted down-regulated after 21 and 28 days of differentiation. On the opposite the synapsis-related genes SYP and MAPT (Figure 2K) were significantly upregulated upon differentiation, while GFAP, expressed by glial cells did not significantly change and its overall expression resulted very low or absent (Figure 2K). These results suggest either that the culture conditions and the neuronal differentiation protocol recommended by the manufacturer (PhenoCell) are not sufficiently optimized (e.g., possible issues with cell plating density) and/or that insertion of Nrf2/Luciferase construct could have modified the neuronal differentiation capacity of these cells. Additional experiments were done in an effort to optimize the culture conditions and improve the differentiation efficiency of Cl27 cells, particularly by (i) reducing the cell plating density (from 50.000 to 25.000 cells/cm^2), and (ii) by adding retinol (vitamin A, contained in the classic B27 supplement), but without significant differences (data not shown).

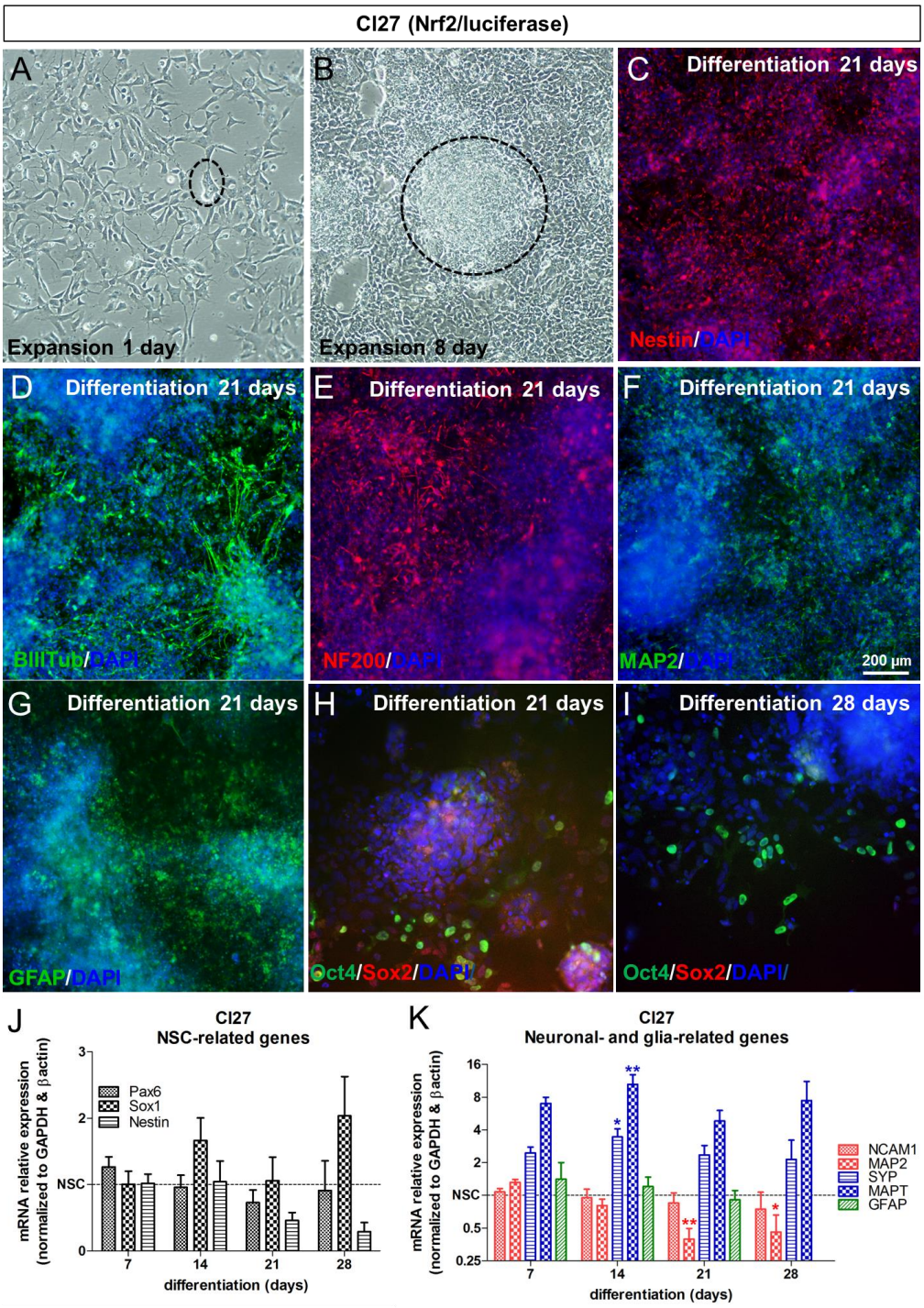

Figure 2. Analysis of neuronal and glial differentiation potential of Cl27 cells. (A, B) Cl27 cells could be efficiently expanded using manufacturer's protocol; however, PSC-like cells resulted visible already at early days of expansion and formed highly dense colonies along the course of time (dashed circles). (C-I) Representative images of Cl27 cells differentiated for 21 days and stained for Nestin (red), B-III-tubulin (green), NF200 (red), MAP2 (green), GFAP (green), Oct4 (green), Sox2 (red), and counterstained with DAPI. Cl27 cells continued to proliferate over time, without generating fully mature neuronal networks. This was also confirmed by analysis of NSC markers nestin (C) that resulted expressed in nearly all cells, and Sox2 (H), while some cells resulted positive for the PSC marker Oct4 (H, I), even after 28 days of differentiation. Nevertheless, despite their not differentiated morphology, Cl27 cells expressed neuronal markers (B-III-tubulin, MAP2, NF200), and some cells resulted positive for GFAP (indicative of astroglia). (J, K) qPCR analyses of NSC-related genes Pax6, Sox1 and Nestin (J), neuronal related genes NCAM1, MAP2, SYP, MAPT and the glial related gene GFAP (K). Total RNA samples were extracted after 0 (NSCs), 7, 14, 21 and 28 days of differentiation and processed as described in the Methodological approach section. All values were normalized to β-actin and GAPDH and then calibrated to NSCs (undifferentiated cells) (dashed line), ΔΔCt method. All values are shown as mean ± S.E.M. of 3 experiments (* $p < 0,05$, ** $p < 0.01$).

3.1.2 Effect of rotenone on Nrf2 pathway activation in Cl27 cells

Further analyses were carried out to assess at which stage of neuronal/glial differentiation Nrf2 resulted stably expressed in Cl27 cells. To this aim, total RNA were extracted from Cl27 cells differentiated for 0 (i.e., NSCs, calibrating condition), 7, 14, 21 and 28 days, and the expression of the following four Nrf2 target genes was analysed by qPCR: NQO1 (NAD(P)H quinone oxidoreductase 1), playing an important role in quinone metabolism (Li et al., 2013; Tufekci et al., 2011), SRXN1 (sulfiredoxin 1) that catalyses the reversal of overoxidation of peroxiredoxins and deglutathionylation induced by oxidative stress (Tufekci et al., 2011; Zhou et al., 2015), HMOX1 (heme oxygenase-1) that catalyzes the breakdown of heme into biliverdin, carbon monoxide and iron (Kongpetch et al., 2016), and GSR (glutathione reductase) that catalyzes the reduction of glutathione disulfide (GSSG) to the sulfhydryl form glutathione (GSH) (Satoh N et al., 2010). HMOX1 (red bars) resulted significantly upregulated at 14 and 21 days of differentiation, NQO1 (yellow bars) expression resulted modestly increased at 28 days of differentiation, while the expression of both SRXN1 (blue bars) and GSR (green bars) did not change upon differentiation (Figure 3A). These data overall suggest an increase of Nrf2 signalling pathway upon differentiation in Cl27 cells. Accordingly, Nrf2 is known to contribute to diverse cellular functions including differentiation (Bryan et al., 2013).

We sought to evaluate the effects of rotenone treatment in Cl27 cells. Cells at three differentiation stages (i.e., 5, 12 and 19 DIV) were treated with different concentrations of rotenone (i.e., 1, 10, 100, 500, 2500 nM) for either 24 or 72 hr (Figure 3B). The viability rate of cells differentiated for 5 days slightly decreased by about 15% upon 72 hr treatment with 10 nM rotenone (~ IC_{15}) (light grey curve). Cell viability in Cl27 cells differentiated for 12 days (dark grey curve) and 19 days (red curve) dropped by nearly 80-85% with the same concentration (10 nM, ~ IC_{80}-IC_{85}), suggesting that Cl27 cells become more sensitive to rotenone treatment upon differentiation (Figure 3C). These data are not in line with a previous study showing higher sensitivity to rotenone treatment by human NSCs than by their differentiated derivatives, as indicated by analysis of ATP depletion (Li J et al., 2015). The effects here described can be explained considering the low neuronal/glial differentiation potential of Cl27 cells, which keep proliferating even upon mitogen withdrawal and induction of differentiation (Figure 2).

Moreover, we assessed luciferase activity in Cl27 cells treated with either rotenone (using the lowest tested concentration, 1 nM), or H_2O_2 (100 μM, positive control), accounting for solvent DMSO (0.1%) as a negative control. Cells were treated for either 24 or 72 hr, and then processed for the analysis of luciferase as indicated in the Methodological approach. Disappointingly, luciferase/Nrf2 signalling did not increase at any differentiation stages and tested time points with both treatments (i.e., rotenone and H_2O_2). On the opposite, 1 nM rotenone appeared to decrease luciferase activity particularly at later differentiation stages (i.e., 12 and 19 DIV), and the same effect was recorded with H_2O_2 treatment at 19 days of differentiation. Treatment of Cl27 cells with higher concentrations of rotenone (i.e., 10 and 100 nM) at either time points and at all tested differentiation stages analogously decreased luciferase activity (data not shown). These data further confirm that this Nrf2/luciferase reporter cell model is neither suitable as neuronal and glial model, nor can serve to measure Nrf2 activity via luciferase quantification.

For all these reasons we decided to evaluate the effects of rotenone on Nrf2 pathway activity using a well-established and optimized cell culture system, the (wild type) IMR90-hiPSCs, which can be efficiently differentiated into mixed cultures of neuronal and glial cells following previously established protocols (Pistollato et al., 2014; Zagoura et al., 2016).

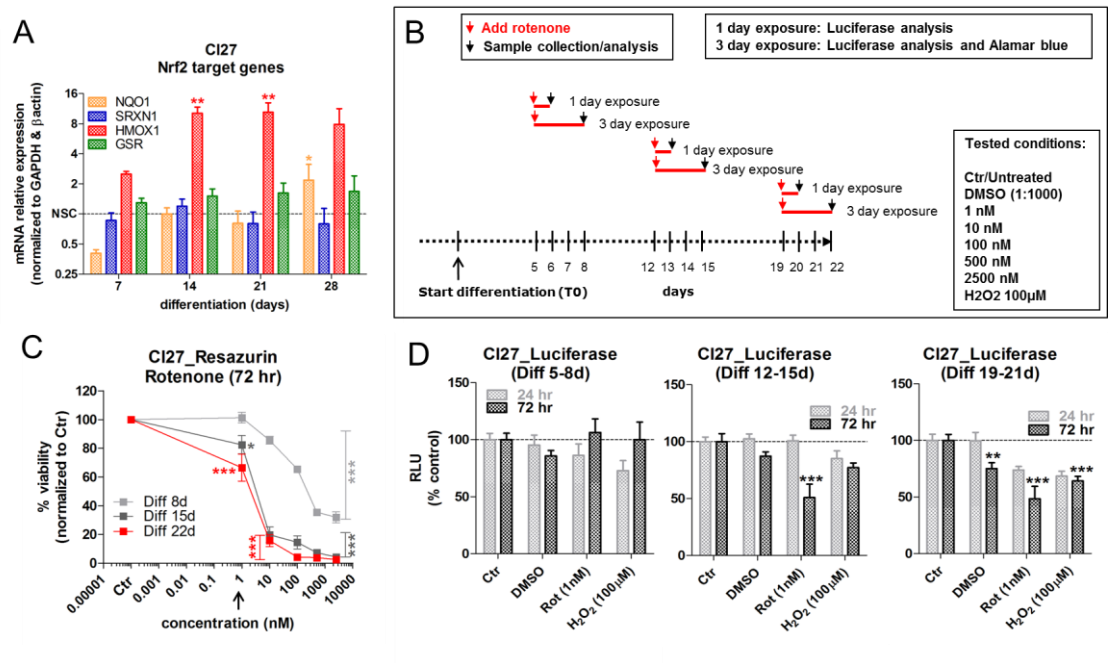

Figure 3. Expression of Nrf2 pathway target genes and effects of rotenone on Nrf2 activity in Cl27 cells. (A) qPCR analyses of the Nrf2-target genes NQO1, SRXN1, HMOX1 and GSR. Total RNA samples were extracted after 0 (NSCs), 7, 14, 21 and 28 days of differentiation and processed as described in the Methodological approach section. All values were normalized to β-actin and GAPDH and then calibrated to NSCs (undifferentiated cells) (dashed line) (ΔΔCt method). (B) Rotenone treatment scheme: Cl27 cells at three differentiation stages (i.e., 5, 12 and 19 days of differentiation) were treated with different concentrations of rotenone (i.e., 1, 10, 100, 500, 2500 nM) for either 24 or 72 hr. Analysis of luciferase (indicative of Nrf2 expression) was done at both time points (i.e., 24 hr and 72 hr), while the Alamar blue assay (resazurin) was performed after 72 hr treatment to evaluate possible cytotoxic effects. H_2O_2 (100 μM) was used as a positive control, and solvent DMSO (0.1%) as a negative control. (C) Alamar blue assay (resazurin): cell viability in Cl27 cells differentiated for 5 days slightly decreased (by about 15%) upon treatment with 10 nM rotenone (~ IC_{15}) (light grey curve); in Cl27 cells differentiated for 12 days (dark grey curve) and 19 days (red curve) viability dropped by nearly 80-85% with the same concentration (10 nM, ~ IC_{80}-IC_{85}), indicating that Cl27 cells result more sensitive to rotenone treatment upon differentiation. (D) Analysis of luciferase: Cl27 cells were treated with either 1 nM rotenone, or H_2O_2 (100 μM, positive control), accounting for solvent DMSO (0.1%) as a negative control. After either 24 or 72 hr, cells were processed for luciferase analysis as indicated in the Methodological approach section. Luciferase/Nrf2 signalling did not increase at any differentiation stages and time points with both treatments (rotenone and H_2O_2). On the opposite, 1 nM rotenone appeared to decrease luciferase signalling particularly at later differentiation stages (12 and 19 days of differentiation), and the same effect was recorded for H_2O_2 treatment at 19 days of differentiation (RLU, relative light unit). Values are shown as mean ± S.E.M. of three biological replicates (* $p < 0,05$, ** $p < 0.01$, *** $p < 0.001$).

3.2 Effects of Rotenone on Nrf2 pathway activation in IMR90-hiPSC-derived neuronal model (wild type)

3.2.1 Neuronal and glial differentiation of IMR90-hiPSCs

IMR90-hiPSCs were directly differentiated into mixed cultures of neuronal and glial cells for 28 days (Figure 4, upper part). In parallel, a protocol for rosette-derived neural stem cell (NSC) expansion and cryopreservation was developed. NSCs could be further differentiated into neurons and glial cells for 21 days (Figure 4, lower part).

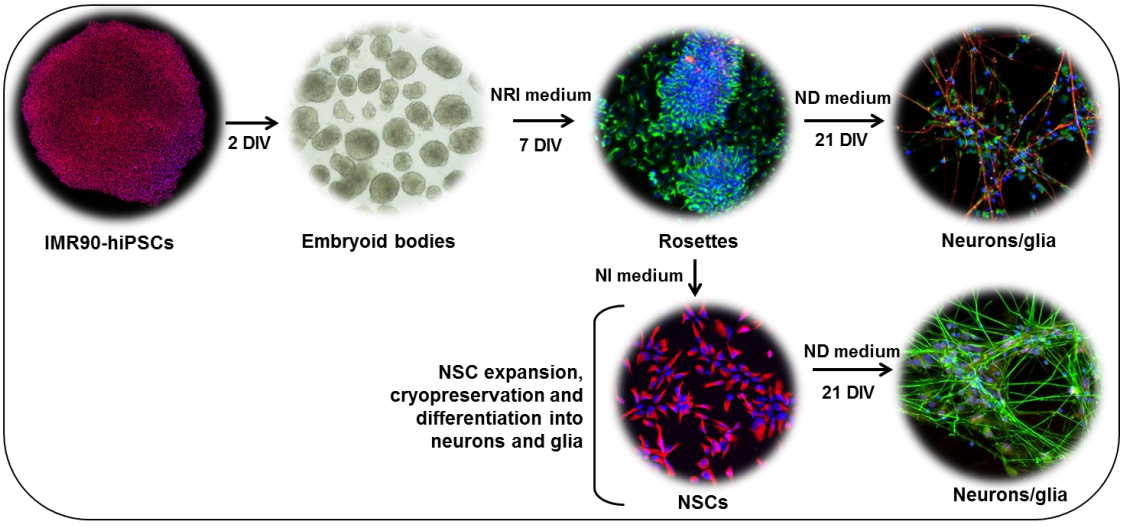

Figure 4. Schematic representation of the neuronal differentiation protocol. (Upper part) IMR90-hiPSC colonies (here stained for Oct4, red) were cut into fragments to form embryoid bodies (EBs, phase bright picture). EBs were plated onto laminin-coated dishes and cultured in the presence of neuroepithelial induction (NRI) medium to generate rosettes (neuroectodermal derivatives, here stained for B-III-tubulin (red) and Nestin (green)), which were further differentiated into mature neuronal (NF200, red) and glial (GFAP, green) cells in the presence of neuronal differentiation (ND) medium. (Lower part) in parallel, a protocol for the expansion and cryopreservation of rosette-derived neural stem cells (NSCs) was developed. NSCs (nestin, red) were expanded in the presence of neural induction (NI) medium or directly differentiated in the presence of ND medium to form mixed neuronal (NF200, green) and glial (GFAP, red) cultures (all cells were counterstained with DAPI). More detailed information about the culture protocols and the characterization of the cellular model used in this study is available at: (Zagoura et al., 2016) and at https://ecvam-dbalm.jrc.ec.europa.eu/methods-and-protocols/protocol/standard-operating-procedure-for-differentiation-of-human-induced-pluripotent-stem-cells-into-post-mitotic-neurons-and-glial-cells-%28mixed-culture%29-protocol-no.-165/key/p_1570 and https://ecvam-dbalm.jrc.ec.europa.eu/methods-and-protocols/protocol/standard-operating-procedure-for-expansion-of-rosette-derived-neural-stem-cells-protocol-no.-166/key/p_1571

Differentiated neuronal-like cells derived from IMR90-hiPSCs expressed high level of the major neuronal cytoskeleton protein, neurofilament 200 (NF200) and about 25-30% of the cells were positive for the glial fibrillary acidic protein (GFAP), marker of astroglia (Zagoura et al., 2016). Similar results were obtained by analyzing neuronal population obtained by expanding rosette-derived NSCs and their further differentiation into neurons (Zagoura et al., 2016). We also found that ~ 25-30% of cells still retained the expression of nestin after differentiation (Zagoura et al., 2016). Furthermore, dopaminergic neurons represented ~ 13-20% of total cell number, GABAergic neurons ~ 15-20%, and glutamatergic neurons ~ 35-42%, as shown by IC analyses of tyrosine hydroxylase (TH), gamma-aminobutyric acid (GABA), and Vesicular Glutamate Transporter 1 (VGlut1) respectively (not shown).

Additionally, differentiated cultures derived from hiPSCs showed neuronal spontaneous electrical activity, with a mean firing rate (MFR) of ~ 293 spikes/minute, and neurons derived from expanded NSCs yielded similar results, with a MFR of ~ 239 spikes/minute (not shown). More detailed information about the culture protocols and the characterization of the cellular model used in this study is described in (Zagoura et al., 2016).

3.2.2 Effect of rotenone on Nrf2 pathway in IMR90-hiPSCs

Rotenone causes oxidative stress by triggering the translocation of Nrf2 from the cytoplasm into the nucleus and Nrf2-ARE target gene transcriptional activation (Tufekci et al. 2011). To evaluate rotenone effects on Nrf2 activation, IMR90-hiPSC-derived neurons and glial cells were exposed to different concentrations of rotenone (1, 10 and 100 nM) for 24 hr (Figure 5A). These concentrations were established according to previous studies (Kovac et al., 2015; Lee et al., 2003). Rotenone did not induce cytotoxicity at these tested concentrations, as shown by morphological analysis and quantification of live DAPI^{+} cell nuclei (Figure 5C).

Induction of Nrf2 nuclear translocation was observed especially after exposing the cells to the highest concentration of rotenone (100 nM) (Figure 5B, D). In parallel, cells exposed to 100 nM rotenone showed a significant decrease of cytoplasmic Keap1 (Kelch-like ECH-associated protein 1) (Figure 5E), a key Nrf2 repressor (Bryan et al., 2013).

Moreover, exposure to 10 and 100 nM rotenone induced a concentration-dependent increase of the Nrf2-target enzymes NQO1 and SRXN1, as shown by immuno-cytochemical analysis (Figure 5F).

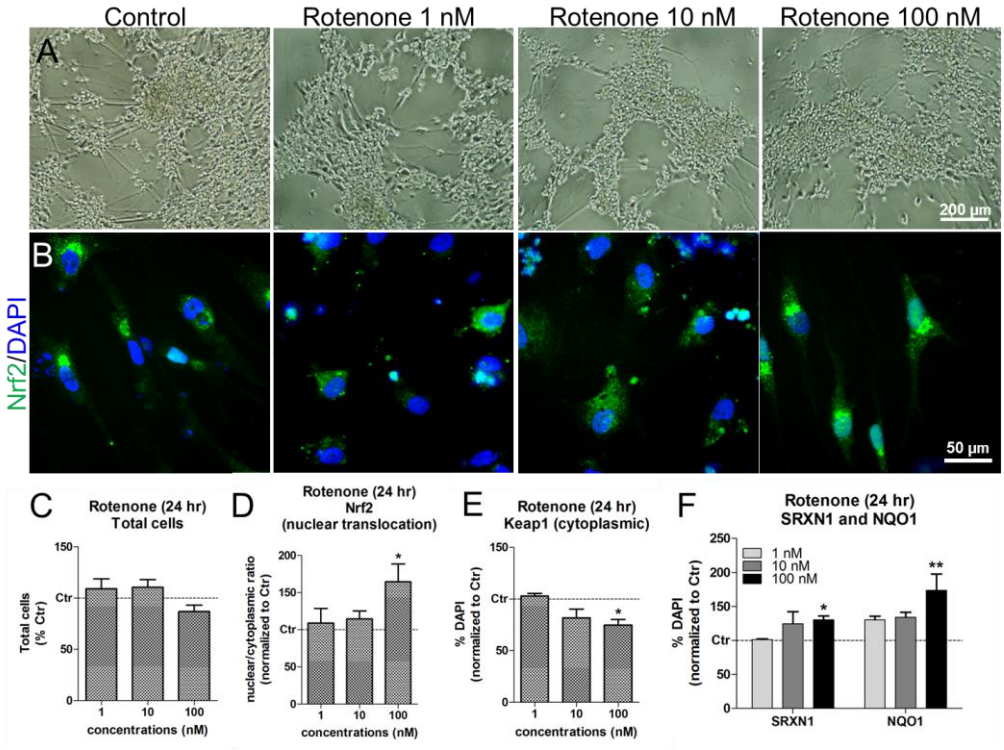

Figure 5. Effects of rotenone on Nrf2 nuclear translocation, Keap1 and antioxidant enzyme levels in IMR90-hiPSCs derived neurons. (A) Representative phase bright images of IMR90-hiPSC-derived neurons treated with 1, 10, 100 nM rotenone for 24 hr. (B) Representative IC images of Nrf2 protein localization (green). (C) Quantification of live DAPI^{+} cells (i.e., non-pyknotic nuclei) upon 24 hr exposure to rotenone (1, 10, 100 nM) and normalized to untreated cells (Ctr). (D) Nrf2 protein nuclear translocation (i.e., nuclear/cytoplasmic ratios) after 24 hr of exposure to rotenone assessed by measurements of fluorescence intensity using HCI analysis. (E) Quantification of cytoplasmic Keap1 protein levels upon rotenone treatment, assessed by HCI analysis. (F) Quantification of NAD(P)H Quinone Oxidoreductase 1 (NQO1) and Sulfiredoxin1 (SRXN1) by means of IC and HCI upon 24 hr treatment with rotenone. All values are shown as mean ± S.E.M. of three biological replicates (* p<0,05, ** p<0.01).

3.2.3 Effect of rotenone on IMR90-hiPSC-derived glial cells and dopaminergic neurons

We further analysed whether rotenone had any effects on the proportion of nestin$^+$, MAP2$^+$ and GFAP$^+$ cells. We found that rotenone increased the percentage of astroglial cells in a concentration-dependent manner, promoting respectively a ~ 46%, ~ 57% and ~ 99% increase in the number of GFAP$^+$ cells compared to control (Figure 6A, C), which was also confirmed by qPCR analysis of GFAP gene expression (not shown). On the contrary, rotenone did not affect the proportions of both nestin$^+$ (NSCs) and MAP2$^+$ cells (neurons) (Figure 6C), which was confirmed also by qPCR analysis (not shown).

Moreover, we found that the number of dopaminergic TH$^+$ neurons was significantly decreased by rotenone treatment, particularly at higher concentrations (i.e., 10 nM and 100 nM) (Figure 6B, D). This is line with previous studies describing a rotenone-dependent and selective dopaminergic neuronal cell death, as shown both in vivo (Cannon et al., 2009; Sherer et al., 2003) and in vitro (Testa et al. 2005). Analysis of GABAergic (GABA$^+$) and glutamatergic (VGlut1$^+$) neurons showed no significant changes upon rotenone treatment (Figure 6D).

Gene expression analysis of GABAergic (GABRA1 and GABRA3), glutamatergic (GRIA1 and GAP43) and dopaminergic (TH and NR4A2) neuronal-related genes revealed no significant variations for GABRA1, GABRA3 and GRIA1 genes, while down-regulation of both GAP43 and NR4A2 (Nurr1) was observed upon rotenone treatment (Figure 6E). Opposite to protein level, TH gene expression resulted significantly increased by rotenone, especially at the highest concentration (100 nM, Figure 6E). TH gene up-regulation by rotenone was also described in PC12 cells (Hohler et al., 1999). This up-regulation could be associated with compensatory mechanisms induced in the surviving cells to recover the reduction of TH protein elicited by rotenone.

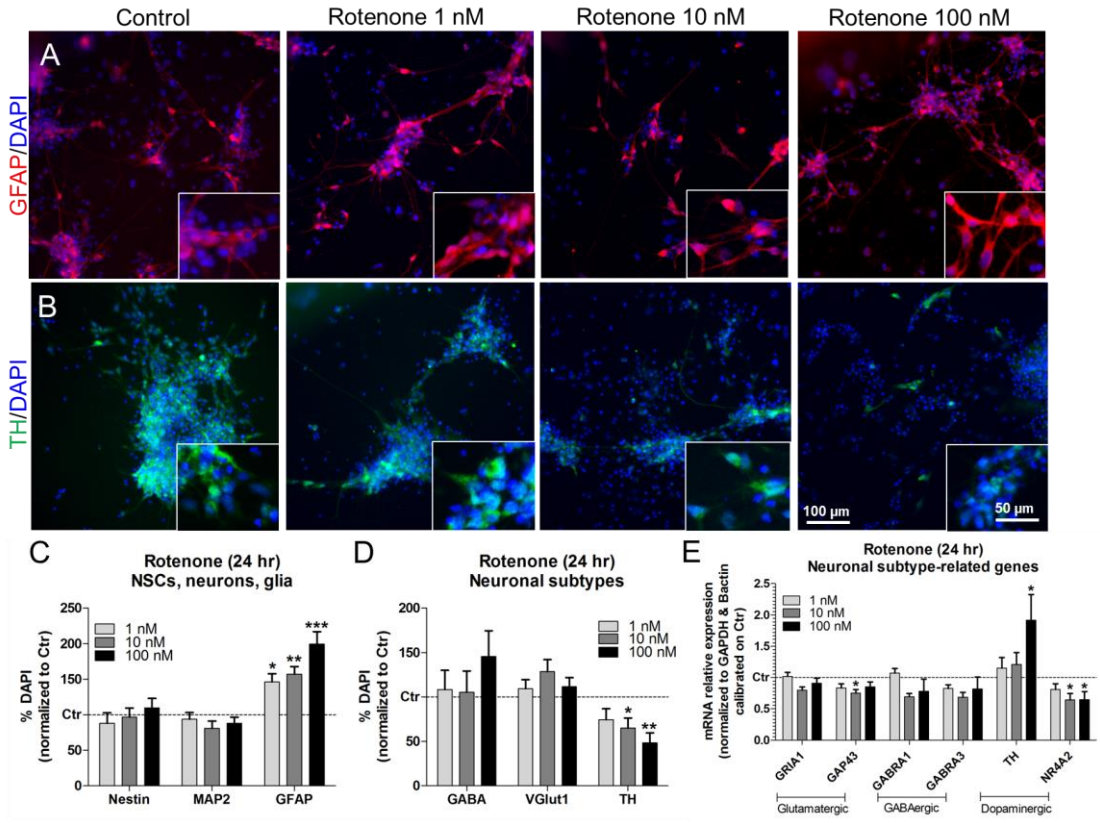

Figure 6. Effects of rotenone on IMR90-hiPSC-derived glial cells and on dopaminergic neurons. (A, B) Representative pictures of GFAP$^+$ cells (red, A), and dopaminergic TH$^+$ neurons (green, B), with 40X magnification insets, left untreated and upon exposure to different concentrations of rotenone (1 nM, 10 nM and 100 nM) for 24 hr. (C, D) Quantification of nestin$^+$, MAP2$^+$, GFAP$^+$ cells (C), and of GABA$^+$, VGlut1$^+$ and TH$^+$ neuronal cells (D) by HCI using the Array Scan vTi platform. (E) qPCR analyses of GRIA1 (Glutamate Ionotropic Receptor AMPA Type Subunit 1), GAP43 (Growth Associated Protein 43), GABRA1 (Gamma-

Aminobutyric Acid Type A Receptor Alpha1 Subunit), GABRA3 (Gamma-Aminobutyric Acid Type A Receptor Alpha3 Subunit), TH (Tyrosine Hydroxylase), NR4A2 (Nuclear Receptor Subfamily 4 Group A Member 2). All values were normalized to β-actin and GAPDH and then calibrated to untreated cells (Ctr, dashed line) (ΔΔCt method). All values are shown as mean ± S.E.M. of three biological replicates (* $p<0,05$, ** $p<0.01$, *** $p<0.001$).

4 Discussion and conclusions

This technical report describes the effects elicited by rotenone on the Nrf2 pathway activation in two models of hiPSC-derived neuronal cultures. However, the results obtained with the Nrf2/luciferase reporter model (named Cl27) have not allowed us to draw clear conclusions about the effects of rotenone on Nrf2 pathway activation. Cl27 cells kept proliferating even upon mitogen (bFGF and EGF) withdrawal and induction of differentiation, and did not form mature neuronal networks. Additionally, treating Cl27 cells with non-cytotoxic concentration of rotenone or with hydrogen peroxide did not increase luciferase activity. These issues could be due to several factors, such as (i) the culture conditions and the neuronal differentiation protocol indicated by the manufacturer (PhenoCell) require further optimization, and/or (ii) the insertion of the Nrf2/luciferase construct has affected the neuronal differentiation capacity of these cells.

Considering these intrinsic limitations, the effects of rotenone on Nrf2 pathway activity were further investigated using a well-established and optimized cell culture system, the IMR90-hiPSCs (wild type). These cells can be efficiently differentiated into mixed cultures of neuronal and glial cells following previously established and optimized protocols (Pistollato et al., 2014; Zagoura et al., 2016).

Differentiated cultures derived from IMR90-hiPSCs or from expanded rosette-derived NSCs were composed of neurons expressing classical neuronal proteins (e.g., NF200 and MAP2) and astrocytes. Astrocytes play an important role in the regulation of oxidative stress defence mechanisms, extracellular glutamate uptake, ions balance, and function of neuronal networks (Barker and Ullian, 2008; Bell et al., 2011; Figley and Stroman, 2011; Santello and Volterra, 2009). Additionally, the adopted neuronal differentiation protocol allowed the formation of different neuronal subtypes (i.e., GABAergic, glutamatergic and dopaminergic neurons), and these neuronal derivatives resulted to be electrically active, as shown by MEA analysis (Zagoura et al., 2016).

Oxidative stress is one of the early effects observed in neuronal cultures exposed to different classes of chemicals, such as rotenone, a known inhibitor of mitochondrial respiration chain (Peng et al., 2013; Satoh et al., 2009). In an effort to maintain homeostasis, neuronal and glial cells respond to chemical insults by activating signalling pathways, such as Nrf2. Nrf2 is known to play a cytoprotective, antioxidant and anti-inflammatory role (Lee et al., 2003; Shih et al., 2005; Tufekci et al., 2011), and is critical in the regulation of cellular defence mechanisms in many body tissues, including the brain (Lee et al., 2003; Shih et al., 2005). Under physiological conditions Nrf2 protein levels are kept low in the cytoplasm due to the rapid proteasome-mediated degradation controlled by the Keap1 protein, an Nrf2-specific ligase adaptor protein (Gorrini et al., 2013; Hartikainen et al., 2012; Harvey et al., 2009; Kansanen et al., 2013). In response to various triggers of oxidative stress, Nrf2 dissociates from Keap1 and translocates into the nucleus (Kovac et al., 2015; Tufekci et al., 2011).

In this report we showed that an acute exposure (24 hr) to rotenone triggered the activation of Nrf2 pathway in IMR90-hiPSC-derived neuronal and glial cultures. In particular, rotenone induced Nrf2 nuclear translocation and a decrease of cytoplasmic Keap1 protein. Moreover, rotenone increased in a concentration-dependent manner NQO1 and SRXN1 protein levels, two enzymes whose expression is controlled by Nrf2 (Itoh et al., 1997; Li et al., 2014), which confirmed the activation of the Nrf2 pathway.

These data indicate that rotenone, by inducing the inhibition of complex I, triggers ROS production and Nrf2 pathway activation (Barrientos and Moraes, 1999). Both NQO1 and SRXN1 protect cells against these effects, as NQO1 catalyzes the reduction of highly reactive quinones, while SRXN1 reduces cysteine-sulfinic acid formed under exposure to oxidants in peroxiredoxins (Ma, 2013).

Additionally, rotenone elicited a dose-dependent increase of GFAP gene expression and protein level, indicative of astrocyte activation (Bal-Price et al., 2010; Cabezas et al., 2012; Swarnkar et al., 2012). Astrocytes are known to respond to different neurological insults (e.g., oxidative stress) by undergoing reactive astrogliosis (Radad et al., 2008; Swarnkar et al., 2012), and astrocytes play a major role in Nrf2-ARE mediated neuroprotection (Johnson et al., 2008).

Importantly, rotenone promoted a decrease in the number of dopaminergic (TH^+) cells. This is in line with previous in vitro and in vivo studies that have shown that rotenone causes a specific dopaminergic neuronal cell death (Testa et al., 2005; Cannon et al., 2009; Sherer et al., 2003). Dopaminergic neurons are particularly sensitive to several stressors, including oxidative stress (Fujita et al., 2014).

Altogether these data indicate that hiPSC-derived neuronal and glial culture models could be valuable to study the neurotoxic effects of chemicals that elicit oxidative stress and activation of the Nrf2 pathway. Oxidative stress is a common key event in various Adverse Outcome Pathways (AOPs) relevant to developmental and adult neurotoxicity (Bal-Price et al., 2015b). Defining key events in AOPs (e.g., Nrf2 pathway activation), could allow assay development for the creation of integrated testing strategies (Bal-Price et al., 2015a), such as AOP-informed IATA (Integrated Approaches to Testing and Assessment) for neurotoxicity testing (Tollefsen et al., 2014), providing mechanistic knowledge suitable to facilitate regulatory decision making process.

The data on the effects of rotenone on the IMR90-hiPSC-neuronal model described in the this technical report have been published in: Zagoura D, Canovas-Jorda D, Pistollato F, Bremer-Hoffmann S, Bal-Price A. 2016. Evaluation of the rotenone-induced activation of the Nrf2 pathway in a neuronal model derived from human induced pluripotent stem cells. Neurochem Int. Sep 9. pii: S0197-0186(16)30284-4.

References

Avior, Y., Sagi, I., Benvenisty, N., 2016. Pluripotent stem cells in disease modelling and drug discovery. Nat Rev Mol Cell Biol.

Bal-Price, A., Crofton, K.M., Leist, M., Allen, S., Arand, M., Buetler, T., Delrue, N., FitzGerald, R.E., Hartung, T., Heinonen, T., Hogberg, H., Bennekou, S.H., Lichtensteiger, W., Oggier, D., Paparella, M., Axelstad, M., Piersma, A., Rached, E., Schilter, B., Schmuck, G., Stoppini, L., Tongiorgi, E., Tiramani, M., Monnet-Tschudi, F., Wilks, M.F., Ylikomi, T., Fritsche, E., 2015a. International STakeholder NETwork (ISTNET): creating a developmental neurotoxicity (DNT) testing road map for regulatory purposes. Arch Toxicol 89, 269-287.

Bal-Price, A., Crofton, K.M., Sachana, M., Shafer, T.J., Behl, M., Forsby, A., Hargreaves, A., Landesmann, B., Lein, P.J., Louisse, J., Monnet-Tschudi, F., Paini, A., Rolaki, A., Schrattenholz, A., Sunol, C., van Thriel, C., Whelan, M., Fritsche, E., 2015b. Putative adverse outcome pathways relevant to neurotoxicity. Crit Rev Toxicol 45, 83-91.

Bal-Price, A.K., Hogberg, H.T., Buzanska, L., Coecke, S., 2010. Relevance of in vitro neurotoxicity testing for regulatory requirements: challenges to be considered. Neurotoxicol Teratol 32, 36-41.

Barker, A.J., Ullian, E.M., 2008. New roles for astrocytes in developing synaptic circuits. Commun Integr Biol 1, 207-211.

Barrientos, A., Moraes, C.T., 1999. Titrating the effects of mitochondrial complex I impairment in the cell physiology. J Biol Chem 274, 16188-16197.

Bell, K.F., Al-Mubarak, B., Fowler, J.H., Baxter, P.S., Gupta, K., Tsujita, T., Chowdhry, S., Patani, R., Chandran, S., Horsburgh, K., Hayes, J.D., Hardingham, G.E., 2011. Mild oxidative stress activates Nrf2 in astrocytes, which contributes to neuroprotective ischemic preconditioning. Proc Natl Acad Sci U S A 108, E1-2; author reply E3-4.

Bryan, H.K., Olayanju, A., Goldring, C.E., Park, B.K., 2013. The Nrf2 cell defence pathway: Keap1-dependent and -independent mechanisms of regulation. Biochem Pharmacol 85, 705-717.

Cabezas, R., El-Bacha, R.S., Gonzalez, J., Barreto, G.E., 2012. Mitochondrial functions in astrocytes: neuroprotective implications from oxidative damage by rotenone. Neurosci Res 74, 80-90.

Cannon, J.R., Tapias, V., Na, H.M., Honick, A.S., Drolet, R.E., Greenamyre, J.T., 2009. A highly reproducible rotenone model of Parkinson's disease. Neurobiol Dis 34, 279-290.

Desbordes, S.C., Studer, L., 2013. Adapting human pluripotent stem cells to high-throughput and high-content screening. Nat Protoc 8, 111-130.

Figley, C.R., Stroman, P.W., 2011. The role(s) of astrocytes and astrocyte activity in neurometabolism, neurovascular coupling, and the production of functional neuroimaging signals. Eur J Neurosci 33, 577-588.

Fujita, K.A., Ostaszewski, M., Matsuoka, Y., Ghosh, S., Glaab, E., Trefois, C., Crespo, I., Perumal, T.M., Jurkowski, W., Antony, P.M., Diederich, N., Buttini, M., Kodama, A., Satagopam, V.P., Eifes, S., Del Sol, A., Schneider, R., Kitano, H., Balling, R., 2014. Integrating pathways of Parkinson's disease in a molecular interaction map. Mol Neurobiol 49, 88-102.

Gorrini, C., Harris, I.S., Mak, T.W., 2013. Modulation of oxidative stress as an anticancer strategy. Nat Rev Drug Discov 12, 931-947.

Hartikainen, J.M., Tengstrom, M., Kosma, V.M., Kinnula, V.L., Mannermaa, A., Soini, Y., 2012. Genetic polymorphisms and protein expression of NRF2 and Sulfiredoxin predict survival outcomes in breast cancer. Cancer Res 72, 5537-5546.

Harvey, C.J., Thimmulappa, R.K., Singh, A., Blake, D.J., Ling, G., Wakabayashi, N., Fujii, J., Myers, A., Biswal, S., 2009. Nrf2-regulated glutathione recycling independent of biosynthesis is critical for cell survival during oxidative stress. Free Radic Biol Med 46, 443-453.

Hohler, B., Lange, B., Holzapfel, B., Goldenberg, A., Hanze, J., Sell, A., Testan, H., Moller, W., Kummer, W., 1999. Hypoxic upregulation of tyrosine hydroxylase gene expression is paralleled, but not induced, by increased generation of reactive oxygen species in PC12 cells. FEBS Lett 457, 53-56.

Hou, Z., Zhang, J., Schwartz, M.P., Stewart, R., Page, C.D., Murphy, W.L., Thomson, J.A., 2013. A human pluripotent stem cell platform for assessing developmental neural toxicity screening. Stem Cell Res Ther 4 Suppl 1, S12.

Itoh, K., Chiba, T., Takahashi, S., Ishii, T., Igarashi, K., Katoh, Y., Oyake, T., Hayashi, N., Satoh, K., Hatayama, I., Yamamoto, M., Nabeshima, Y., 1997. An Nrf2/small Maf heterodimer mediates the induction of phase II detoxifying enzyme genes through antioxidant response elements. Biochem Biophys Res Commun 236, 313-322.

Johnson, J.A., Johnson, D.A., Kraft, A.D., Calkins, M.J., Jakel, R.J., Vargas, M.R., Chen, P.C., 2008. The Nrf2-ARE pathway: an indicator and modulator of oxidative stress in neurodegeneration. Ann N Y Acad Sci 1147, 61-69.

Kansanen, E., Kuosmanen, S.M., Leinonen, H., Levonen, A.L., 2013. The Keap1-Nrf2 pathway: Mechanisms of activation and dysregulation in cancer. Redox Biol 1, 45-49.

Kongpetch S., et al. 2016. Haem oxygenase 1 expression is associated with prognosis in cholangiocarcinoma patients and with drug sensitivity in xenografted mice. Cell Prolif. Feb;49(1):90-101.

Kovac, S., Angelova, P.R., Holmstrom, K.M., Zhang, Y., Dinkova-Kostova, A.T., Abramov, A.Y., 2015. Nrf2 regulates ROS production by mitochondria and NADPH oxidase. Biochim Biophys Acta 1850, 794-801.

Krueger, W.H., Swanson, L.C., Tanasijevic, B., Rasmussen, T.P., 2010. Natural and artificial routes to pluripotency. Int J Dev Biol 54, 1545-1564.

Kumar, K.K., Aboud, A.A., Bowman, A.B., The potential of induced pluripotent stem cells as a translational model for neurotoxicological risk. Neurotoxicology 33, 518-529.

Lee, J.M., Shih, A.Y., Murphy, T.H., Johnson, J.A., 2003. NF-E2-related factor-2 mediates neuroprotection against mitochondrial complex I inhibitors and increased concentrations of intracellular calcium in primary cortical neurons. J Biol Chem 278, 37948-37956.

Li J, Spletter ML, Johnson DA, Wright LS, Svendsen CN, Johnson JA. 2005. Rotenone-induced caspase 9/3-independent and -dependent cell death in undifferentiated and differentiated human neural stem cells. J Neurochem. Feb;92(3):462-76.

Li, L., Dong, H., Song, E., Xu, X., Liu, L., Song, Y., 2013. Nrf2/ARE pathway activation, HO-1 and NQO1 induction by polychlorinated biphenyl quinone is associated with reactive oxygen species and PI3K/AKT signaling. Chem Biol Interact 209, 56-67.

Ma, Q., 2013. Role of nrf2 in oxidative stress and toxicity. Annu Rev Pharmacol Toxicol 53, 401-426.

Nandipati, S., Litvan, I. 2016. Environmental Exposures and Parkinson's Disease. Int J Environ Res Public Health. Sep 3;13(9). pii: E881.

O'Brien, P.J., Irwin, W., Diaz, D., Howard-Cofield, E., Krejsa, C.M., Slaughter, M.R., Gao, B., Kaludercic, N., Angeline, A., Bernardi, P., Brain, P., Hougham, C., 2006. High concordance of drug-induced human hepatotoxicity with in vitro cytotoxicity measured in a novel cell-based model using high content screening. Arch Toxicol 80, 580-604.

Peng, J., Liu, Q., Rao, M.S., Zeng, X., 2013. Using human pluripotent stem cell-derived dopaminergic neurons to evaluate candidate Parkinson's disease therapeutic agents in MPP+ and rotenone models. J Biomol Screen 18, 522-533.

Pistollato, F., Bremer-Hoffmann, S., Healy, L., Young, L., Stacey, G., 2012. Standardization of pluripotent stem cell cultures for toxicity testing. Expert Opin Drug Metab Toxicol 8, 239-257.

Pistollato, F., Louisse, J., Scelfo, B., Mennecozzi, M., Accordi, B., Basso, G., Gaspar, J.A., Zagoura, D., Barilari, M., Palosaari, T., Sachinidis, A., Bremer-Hoffmann, S., 2014. Development of a pluripotent stem cell derived neuronal model to identify chemically induced pathway perturbations in relation to neurotoxicity: effects of CREB pathway inhibition. Toxicol Appl Pharmacol 280, 378-388.

Radad, K., Gille, G., Rausch, W.D., 2008. Dopaminergic neurons are preferentially sensitive to long-term rotenone toxicity in primary cell culture. Toxicol In Vitro 22, 68-74.

Ramsey, C.P., Glass, C.A., Montgomery, M.B., Lindl, K.A., Ritson, G.P., Chia, L.A., Hamilton, R.L., Chu, C.T., Jordan-Sciutto, K.L., 2007. Expression of Nrf2 in neurodegenerative diseases. J Neuropathol Exp Neurol 66, 75-85.

Robinton, D.A., Daley, G.Q., 2012. The promise of induced pluripotent stem cells in research and therapy. Nature 481, 295-305.

Santello, M., Volterra, A., 2009. Synaptic modulation by astrocytes via Ca2+-dependent glutamate release. Neuroscience 158, 253-259.

Satoh N, Watanabe N, Kanda A, Sugaya-Fukasawa M, Hisatomi H. 2010. Expression of glutathione reductase splice variants in human tissues. Biochem Genet. Oct;48(9-10):816-21.

Satoh, T., Harada, N., Hosoya, T., Tohyama, K., Yamamoto, M., Itoh, K., 2009. Keap1/Nrf2 system regulates neuronal survival as revealed through study of keap1 gene-knockout mice. Biochem Biophys Res Commun 380, 298-302.

Sherer, T.B., Kim, J.H., Betarbet, R., Greenamyre, J.T., 2003. Subcutaneous rotenone exposure causes highly selective dopaminergic degeneration and alpha-synuclein aggregation. Exp Neurol 179, 9-16.

Shih, A.Y., Imbeault, S., Barakauskas, V., Erb, H., Jiang, L., Li, P., Murphy, T.H., 2005. Induction of the Nrf2-driven antioxidant response confers neuroprotection during mitochondrial stress in vivo. J Biol Chem 280, 22925-22936.

Sun, Z., Zhang, S., Chan, J.Y., Zhang, D.D., 2007. Keap1 controls postinduction repression of the Nrf2-mediated antioxidant response by escorting nuclear export of Nrf2. Mol Cell Biol 27, 6334-6349.

Swarnkar, S., Singh, S., Goswami, P., Mathur, R., Patro, I.K., Nath, C., 2012. Astrocyte activation: a key step in rotenone induced cytotoxicity and DNA damage. Neurochem Res 37, 2178-2189.

Testa, C.M., Sherer, T.B., Greenamyre, J.T., 2005. Rotenone induces oxidative stress and dopaminergic neuron damage in organotypic substantia nigra cultures. Brain Res Mol Brain Res 134, 109-118.

Tollefsen, K.E., Scholz, S., Cronin, M.T., Edwards, S.W., de Knecht, J., Crofton, K., Garcia-Reyero, N., Hartung, T., Worth, A., Patlewicz, G., 2014. Applying Adverse Outcome Pathways (AOPs) to support Integrated Approaches to Testing and Assessment (IATA). Regul Toxicol Pharmacol 70, 629-640.

Tufekci, K.U., Civi Bayin, E., Genc, S., Genc, K., 2011. The Nrf2/ARE Pathway: A Promising Target to Counteract Mitochondrial Dysfunction in Parkinson's Disease. Parkinsons Dis 2011, 314082.

Yap, M.S., Nathan, K.R., Yeo, Y., Lim, L.W., Poh, C.L., Richards, M., Lim, W.L., Othman, I., Heng, B.C., Neural Differentiation of Human Pluripotent Stem Cells for Nontherapeutic Applications: Toxicology, Pharmacology, and In Vitro Disease Modeling. Stem Cells Int 2015, 105172.

Zagoura D, Canovas-Jorda D, Pistollato F, Bremer-Hoffmann S, Bal-Price A. 2016. Evaluation of the rotenone-induced activation of the Nrf2 pathway in a neuronal model derived from human induced pluripotent stem cells. Neurochem Int. Sep 9. pii: S0197-0186(16)30284-4.

Zhou, Y., Duan, S., Zhou, Y., Yu, S., Wu, J., Wu, X., Zhao, J., Zhao, Y., 2015. Sulfiredoxin-1 attenuates oxidative stress via Nrf2/ARE pathway and 2-Cys Prdxs after oxygen-glucose deprivation in astrocytes. J Mol Neurosci 55, 941-950.

List of abbreviations and definitions

AOPs, Adverse Outcome Pathways

ARE, Antioxidant-Responsive-Element

GABA, Gamma-Aminobutyric Acid

GABRA1, Gamma-Aminobutyric Acid Type A Receptor Alpha1 Subunit

GABRA3, Gamma-Aminobutyric Acid Type A Receptor Alpha3 Subunit

GAP43, Growth Associated Protein 43

GAPDH, Glyceraldehyde 3-phosphate dehydrogenase

GFAP, Glial Fibrillary Acidic Protein

GSR, Glutathione Reductase

GRIA1, Glutamate Ionotropic Receptor AMPA Type Subunit 1

HCI, High Content Imaging

hESCs, Human Embryonic Stem Cells

hiPSCs, Human Induced Pluripotent Stem Cells

HMOX1, Heme Oxygenase-1

IATA, Integrated Approaches to Testing and Assessment

Keap1, Kelch-like ECH-Associated Protein 1

MAP2, Microtubule-Associated Protein 2

MEA, Multi Electrode Array

MFR, Mean Firing Rate

NF200, Neurofilament 200

NQO1, NAD(P)H Quinone Oxidoreductase 1

NR4A2, Nuclear Receptor Subfamily 4 Group A Member 2

Nrf2, Nuclear Factor (erythroid-derived 2)-like 2

NSCs, Neural Stem Cells

Pax6, Paired Box 6

PSCs, Pluripotent Stem Cells

SRXN1, Sulfiredoxin1

TH, Tyrosine Hydroxylase

VGlut1, Vesicular Glutamate Transporter 1

List of figures

LA-NA-28172-EN-N

JRC Mission

As the science and knowledge service of the European Commission, the Joint Research Centre's mission is to support EU policies with independent evidence throughout the whole policy cycle.

EU Science Hub
ec.europa.eu/jrc

@EU_ScienceHub
EU Science Hub - Joint Research Centre
Joint Research Centre
EU Science Hub

Publications Office

doi:10.2787/36841
ISBN 978-92-79-63194-8